

# Camera-supervised Monitor Shading Correction for Softproofing Systems

Johannes Brauers<sup>(a)</sup>, Julie Klein<sup>(a)</sup>, Bernhard Hill<sup>(b)</sup> and Til Aach<sup>(a)</sup>

<sup>(a)</sup>Institute of Imaging & Computer Vision, RWTH Aachen University, Templergraben 55, D-52056 Aachen, Germany

<sup>(b)</sup>Color and Image Processing Research Group, RWTH Aachen University, Templergraben 55, D-52056 Aachen, Germany

## Abstract

A softproofing system is required to faithfully display color images. As the user relies on an appropriate calibration of the system, a method for the evaluation of the quality of the calibration is required. Such a method has recently been developed and allows a critical side-by-side comparison between the original sample and the reproduced monitor image by placing the original directly in front of the monitor. An internal light source of the softproofing system establishes an almost uniform illumination of the target.

In this paper, we present a method to spatially equalize the brightness of the monitor with respect to an object placed in front of the monitor. The automatic calibration procedure requires minimal user intervention and utilizes a standard RGB camera in combination with a special calibration target. The results show that the camera enables an accurate and uncomplicated homogenization of the monitor with respect to the object in front of the monitor.

## Introduction

High-end monitors exhibit a homogenized image reproduction by either factory-provided equalization tables or a user-driven measurement: The latter asks the user to measure several positions on the monitor's surface with a colorimetric or spectral measurement device. The measured values are stored in the monitor's internal memory and are applied to the images to achieve a uniform image representation. We call this monitor equalization an "absolute calibration". However, if a side-by-side comparison with objects, which are placed directly adjacent to the monitor, and their reproduced images is desired, there appear at least brightness differences between the original and the reproduction. This is because the ambient illumination does in most cases not ensure a homogeneous lighting on the monitor's surface or on the object. We therefore apply a "relative calibration", where the monitor's brightness is adapted to the illumination on the monitor's surface.

In the literature, several papers are found describing a monitor calibration with respect to color, i.e., they describe a mathematical relation between the RGB values of the monitor and XYZ values to be reproduced [1, 2]. In this paper, the focus is on the equalization of the brightness of the monitor with respect to the illumination on the monitor's surface and not on the colorimetric calibration. Information on the color calibration is given in [3].

In the following section, we will give some details about the specific softproofing system used in this contribution. We then describe our algorithm, which is divided into three parts – finding a geometric relation between the camera image and the monitor image, a detection of the calibration mask and the final calibration process. After the results, we finally conclude the paper.



**Figure 1.** The softproofing system with its built-in illumination at the top side makes a critical side-by-side comparison between objects and their reproduction on the monitor feasible.

## Background and Model

Fig. 1 shows a new kind of softproofing system [4, 3]: Objects in front of the monitor are illuminated accurately by the integrated light source of the cabin. The black level of the monitor, i.e., the darkest displayable color, is not increased as a result of an appropriate design of the cabin and a low reflectance of the monitor's surface. The additional illumination allows the objects to be placed directly beneath the reproduced image. This makes a direct comparison between the original and the image reproduced on the monitor possible and allows for very precise comparisons in contrast to other softproofing systems: Since the user is not required to change the viewing position as it would be the case when using a separate cabin for the original, the colors can be compared directly.

An important condition to make such a comparison meaningful is the spatial equalization of the brightness levels of both the illuminated original and its reproduced image on the monitor. For calibration, a calibration target as shown in Fig. 2 is required: The cut-outs in this target enable to view the original monitor image, whereas the surrounding white template areas represent the brightness of the illumination at the corresponding positions and make a direct comparison with the inner areas possible.

Brightness differences between the monitor and the illuminated test target with cut-outs are caused by the following issues: The monitor may exhibit a non-homogeneous background illumination causing, e.g., darker shades on the borders. Additionally, although the light source in Fig. 1 has been optimized with a special aperture [3] to produce a homogeneous illumination on the monitor's surface, a perfectly constant brightness across the monitor screen has not been achieved yet.

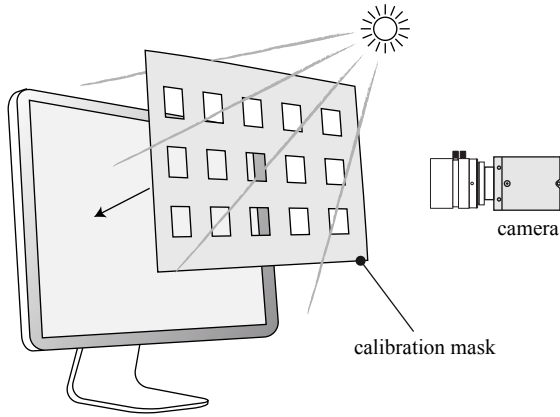


**Figure 2.** The camera aims at the display and is placed approximately at the same position as a human viewer watching the display.

Fig. 3 shows a detailed view of the calibration mask from Fig. 2: The cut-outs of the calibration mask let the monitor image show through. The monitor is assumed to have a constant spectrum  $\mathbf{E} = r\mathbf{R} + g\mathbf{G} + b\mathbf{B}$  at the area of one cut-out, where  $\mathbf{R}$ ,  $\mathbf{G}$  and  $\mathbf{B}$  are the monitor primaries given in a discretized form with  $N$  spectral sampling values in a column vector. The scalars  $r$ ,  $g$  and  $b$  are the linear monitor values for these three primaries at the position behind this specific cut-out. Since the reflectance of the monitor's surface under the given configuration in Fig. 1 is very low, we do not incorporate the reflection of the built-in light source at the monitor's surface for computation of the color stimulus present at the cut-outs. The spectrum outside the cut-out is given by  $\varphi = \text{diag}(\mathbf{S})\boldsymbol{\beta}$ , where  $\mathbf{S}$  is the spectral distribution of the built-in light source and  $\boldsymbol{\beta} \in \mathbb{R}^{N \times 1}$  is the reflectance factor vector of the calibration mask. The operation  $\text{diag}()$  is a diagonalization.

In terms of this mathematical description, our aim is to adjust the monitor levels  $r$ ,  $g$  and  $b$  in such a way that the color impression for human viewers is the same for the regions inside and outside of each specific cut-out area. This is specified with

$$\mathbf{T}_{xyz}\boldsymbol{\varphi} = \mathbf{T}_{xyz}(r\mathbf{R} + g\mathbf{G} + b\mathbf{B}), \quad (1)$$

where  $\mathbf{T}_{xyz} \in \mathbb{R}^{3 \times N}$  is the matrix form of the standard observer [5] with  $N$  spectral sampling values. By rewriting Eq. (1), we get

$$\begin{aligned} \mathbf{T}_{xyz}\boldsymbol{\varphi} &= \mathbf{T}_{xyz}(\mathbf{R} \ \mathbf{G} \ \mathbf{B})(r \ g \ b)^T \\ &= \mathbf{T}_{\text{rgbxyz}}(r \ g \ b)^T = \mathbf{T}_{\text{rgbxyz}}\mathbf{v}_{\text{rgb}}, \end{aligned} \quad (2)$$

where  $\mathbf{T}_{\text{rgbxyz}} = \mathbf{T}_{xyz}(\mathbf{R} \ \mathbf{G} \ \mathbf{B})$  and  $\mathbf{v}_{\text{rgb}} = (r \ g \ b)^T$ . To achieve a homogeneous brightness between the regions inside and outside the cut-out area, we have to display the trichromatic monitor vector

$$\mathbf{v}_{\text{rgb}} = \mathbf{T}_{\text{rgbxyz}}^{-1} \mathbf{T}_{xyz}\boldsymbol{\varphi}. \quad (3)$$

Since the amplitude of the color stimulus  $\boldsymbol{\varphi}$  varies over the surface on the monitor due to illumination inhomogeneities and since the primaries of the monitor might not be constant in their amplitude for each position on the monitor, we theoretically would have to perform the measurement of  $\boldsymbol{\varphi}$  at each position on the calibration mask. Instead, our approach is to calibrate the system using an RGB camera: We set up an equation similar to

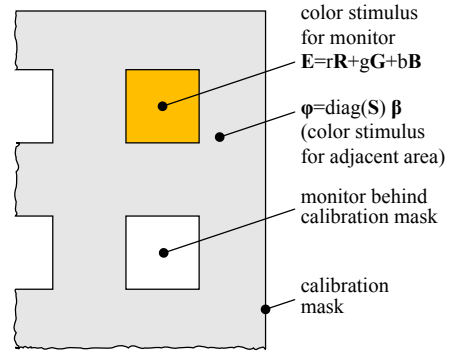


**Figure 3.** Detailed view of the calibration mask: Our aim is to adjust the monitor gray levels  $r, g, b$  so that  $\mathbf{T}_{\text{cam}}\mathbf{E} = \mathbf{T}_{\text{cam}}\boldsymbol{\varphi}$  holds, i.e., the camera values are the same for the region inside and outside the cut-outs.

Eq. (1)

$$\begin{aligned} \mathbf{T}_{\text{cam}}\boldsymbol{\varphi} &= \mathbf{T}_{\text{cam}}(r'\mathbf{R} + g'\mathbf{G} + b'\mathbf{B}) \\ &= \mathbf{T}_{\text{camrgb}}\mathbf{v}'_{\text{rgb}}, \end{aligned} \quad (4)$$

by using the camera sensitivity matrix  $\mathbf{T}_{\text{cam}} \in \mathbb{R}^{3 \times N}$  instead of the human observer matrix  $\mathbf{T}_{xyz}$ , a new combined matrix  $\mathbf{T}_{\text{camrgb}} \in \mathbb{R}^{3 \times 3}$  and a new vector  $\mathbf{v}'_{\text{rgb}}$  for the monitor levels. We derive a solution for the trichromatic monitor vector

$$\mathbf{v}'_{\text{rgb}} = \mathbf{T}_{\text{camrgb}}^{-1} \mathbf{T}_{\text{cam}}\boldsymbol{\varphi}. \quad (5)$$

At this point,  $\mathbf{v}'_{\text{rgb}}$  is computed in such a way that the regions inside and outside the cut-out area match for the camera, whereas  $\mathbf{v}_{\text{rgb}}$  in Eq. (3) enables a matching for the standard observer. Since the primaries of the monitor and the spectrum of the external light source do not change, we can derive a relation between both vectors via

$$\mathbf{v}'_{\text{rgb}} = \mathbf{T}_{\text{ad}}\mathbf{v}_{\text{rgb}}, \quad (6)$$

where  $\mathbf{T}_{\text{ad}} \in \mathbb{R}^{3 \times 3}$  is a diagonal transformation matrix. Finally, this allows us to perform the matching of the areas inside and outside the cut-out areas by using a camera and to convert the resulting RGB values  $\mathbf{v}'_{\text{rgb}}$  to values which allow a match for the human observer. The estimation of the matrix  $\mathbf{T}_{\text{ad}}$  can be realized by performing the adjustment between the areas inside and outside the cut-out areas for the human viewer (see Eq. (2)) as well as the camera (see Eq. (4)). The matrix  $\mathbf{T}_{\text{ad}}$  can then be derived from Eq. (6).

By inserting Eq. (3) and Eq. (5) into Eq. (6), we derive

$$\mathbf{T}_{\text{camrgb}}^{-1} \mathbf{T}_{\text{cam}}\boldsymbol{\varphi} = \mathbf{T}_{\text{ad}}\mathbf{T}_{\text{rgbxyz}}^{-1} \mathbf{T}_{xyz}\boldsymbol{\varphi}. \quad (7)$$

This equation is true for the following three assumptions: First, the primaries of the monitor  $\mathbf{R}$ ,  $\mathbf{G}$  and  $\mathbf{B}$  do not change (although their control values vary). Second, the spectral sensitivity curves of the camera and the color matching function are constant. Third, the spectral shape of color stimulus  $\boldsymbol{\varphi}$  does not change. A variation of the amplitude of  $\boldsymbol{\varphi} = \alpha\boldsymbol{\varphi}'$  cancels out in Eq. (7) since  $\alpha$  a scalar. However, in practice, there might be more complicated effects in the human visual system, which are not modeled by the above equations.

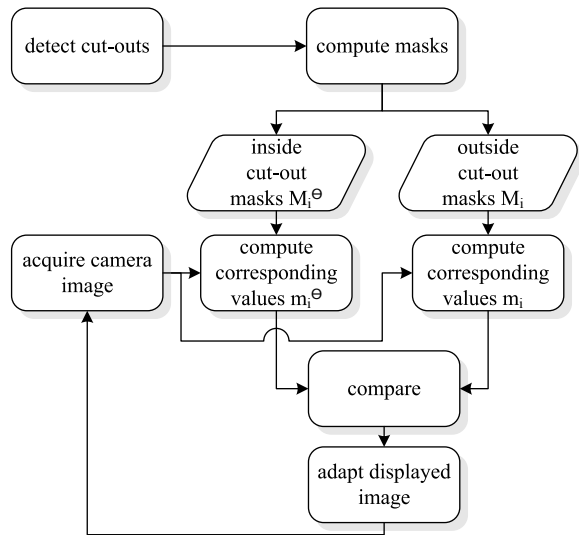


Figure 4. Calibration procedure as described in the text.

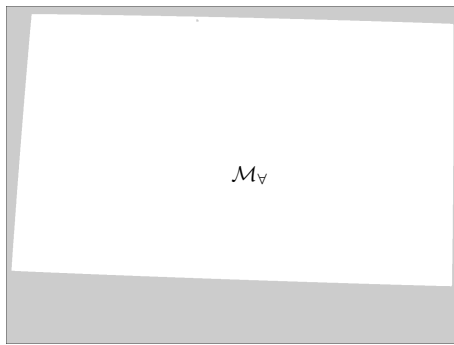


Figure 5. The binary mask  $\mathcal{M}_v$  for the monitor image.

## Calibration Procedure

### Relation Between Monitor Coordinates and Camera Coordinates

The goal of the calibration procedure is to adapt the gray levels of the monitor in the cut-out areas (see Fig. 2) to match their surrounding areas illuminated by the integrated light source of the softproofing system. To automate the gray level adaption procedure, a camera is placed at approximately the same position as a human viewer is normally looking at the display (see Fig. 2). Since it is infeasible to place the camera in such a way that the pixels of the monitor are mapped one by one to the pixels of the camera, a geometric relation has to be computed between the pixel coordinates  $(x_{\text{mon}}, y_{\text{mon}})^T$  of the image displayed on the monitor and the coordinates  $(x_{\text{cam}}, y_{\text{cam}})^T$  of the image taken by the camera (see Fig. 6).

The complete calibration procedure is illustrated in Fig. 4: The exposure time of the camera is first adjusted to produce no clipping when the monitor image is set to full brightness. To compute the position of the monitor in the camera image, the image displayed on the monitor is set sequentially to a black and to a white level and the camera acquires an image of the monitor each time. Doing so, practically the only differences between both acquired images is the display area of the monitor switched from zero to full brightness. The differences of the pixel values between both images are therefore computed and a threshold operation [6] is applied to the image to retrieve the binary mask

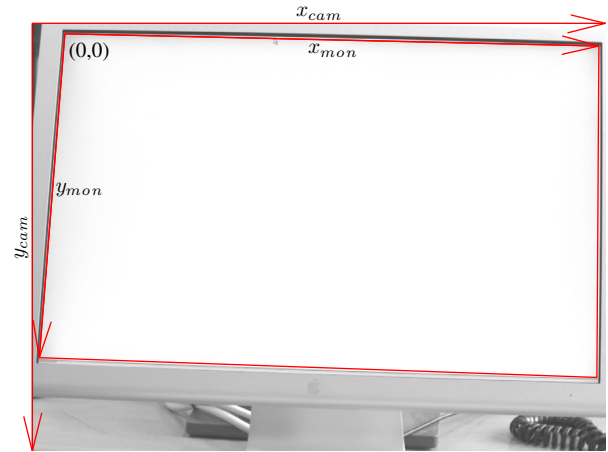


Figure 6. The acquired monitor image as seen by the camera.

shown in Fig. 5.

Since there might be other disturbing objects in the scene which differ between both acquired images and furthermore, the image might be compromised by noise, the binary mask has to be further processed. A morphological opening operation [7] is therefore applied, which removes single, non-connected points from the image. After this step, the improved binary mask typically shows the position of the monitor as a connected region and perhaps some other, smaller regions corresponding to other objects in the scene whose gray values have not been constant between the two acquired images. To distinguish the monitor from other objects detected by mistake, all regions are analyzed with respect to their area. Finally, the largest region is assumed to be the one corresponding to the monitor (see Fig. 6). This region is termed  $\mathcal{M}_v$ ; if other regions are present in the image, they are discarded.

The four corners of the region  $\mathcal{M}_v$  are then detected in the image acquired by the camera and are given in camera coordinates  $(x_{\text{cam}}, y_{\text{cam}})^T$  (see Fig. 6). Each corner of this region corresponds to one corner of the physical monitor. A mathematical relation between the coordinates of the corners in both coordinate systems is given by the following projective transformation

$$\begin{pmatrix} u & v & w \end{pmatrix}^T = \mathbf{M} \begin{pmatrix} x_{\text{cam}} & y_{\text{cam}} & 1 \end{pmatrix}^T \quad (8)$$

and

$$x_{\text{mon}} = \frac{u}{w}, \quad y_{\text{mon}} = \frac{v}{w}, \quad (9)$$

where  $\mathbf{M}$  is a projective transformation matrix [8] of size  $3 \times 3$ . Each position in the camera image within the monitor region  $\mathcal{M}_v$  can now be traced back to the original monitor position.

### Detection of Cut-Out Areas and Masking

The cut-out areas in the special calibration target in Fig. 2 are detected in the same manner as described in the previous section to find the monitor's position. The calibration target with the cut-outs is placed on the monitor's surface. A black and a white image are then sequentially displayed on the monitor and a camera image is acquired for each of these. The difference between both acquired images is computed and shows the position of the cut-outs. A postprocessing similar to the one described above is then applied to the difference image to improve the resulting binary mask. Each cut-out region is labeled with its own index  $i$  (see Fig. 7) and will be described by  $\mathcal{M}_i$  in the following. Since



**Figure 7.** The cut-out areas  $\mathcal{M}_i$  are numbered for the subsequent calibration process.

we are only interested in the regions inside the monitor's area  $\mathcal{M}_V$  in the camera image, we exclude areas outside the monitor area mask  $\mathcal{M}_V$  and thus conform to

$$\mathcal{M}_i \subseteq \mathcal{M}_V. \quad (10)$$

An overview over the following calibration procedure is illustrated in Fig. 4: After the detection of the cut-out regions  $\mathcal{M}_i$  above, two masks  $\mathcal{M}_i^\ominus$  and  $\mathcal{M}_i^\oplus$  are computed for each region  $\mathcal{M}_i$ . The mask  $\mathcal{M}_i^\ominus$  is used to select the region inside the cut-out area for measuring the brightness of the monitor at this position and  $\mathcal{M}_i^\oplus$  is used to measure the surrounding brightness on the calibration target, which depends on the specific illumination. The regions

$$\mathcal{M}_i^\ominus = \mathcal{M}_i \ominus F_1 \quad (11)$$

are utilized to measure the brightness of the monitor in the cut-out areas of the camera image. They are derived from the original regions  $\mathcal{M}_i$  by applying an erosion operation  $\ominus$  with the structuring element  $F_1$  – the resulting regions  $\mathcal{M}_i^\ominus$  are therefore smaller. The erosion is performed to ensure that the measurement of the brightness is performed inside the area and that border effects at the edges of the cut-outs are excluded. The average brightness of one cut-out area  $\mathcal{M}_i^\ominus$  is computed via

$$m_i^\ominus = \frac{1}{|\mathcal{M}_i^\ominus|} \sum_{\mathcal{M}_i^\ominus} I, \quad (12)$$

where  $|\mathcal{M}_i^\ominus|$  is the cardinality of  $\mathcal{M}_i^\ominus$ , i.e., the number of elements in the corresponding region and the sum applies to all elements of the image  $I$ , which are addressed by  $\mathcal{M}_i^\ominus$ .

The brightness of the surrounding of a particular region  $\mathcal{M}_i$  is selected with

$$\mathcal{M}_i^\oplus = \mathcal{M}_i \oplus F_2 - \mathcal{M}_i \oplus F_1, \quad (13)$$

where  $F_2$  is a structuring element larger than the structuring element  $F_1$  used in Eq. (11) and the operation  $\oplus$  is a dilation operation. By subtracting both dilated areas  $\mathcal{M}_i \oplus F_2$  and  $\mathcal{M}_i \oplus F_1$  in Eq. (13), a small border around the original cut-out region is retrieved as shown in Fig. 8. This allows a measurement of the brightness on the calibration target close to the original cut-out

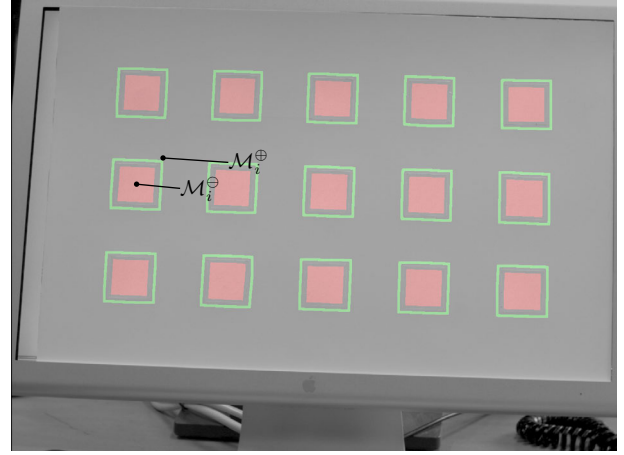


**Figure 8.** Different masks used for calibration: The mask  $\mathcal{M}_i^\ominus$  is used to measure the brightness of the monitor inside the cut-out areas and the mask  $\mathcal{M}_i^\oplus$  is used to measure the surrounding brightness.

area, but with a small distance to the border of that area to prevent border effects. Again, the mean pixel value of the area  $\mathcal{M}_i^\oplus$  can be computed via

$$m_i^\oplus = \frac{1}{|\mathcal{M}_i^\oplus|} \sum_{\mathcal{M}_i^\oplus} I. \quad (14)$$

### Adjustment of Gray Levels

Now the camera values  $m_i^\ominus$  correspond to the brightness inside the cut-out regions and the values  $m_i^\oplus$  represent the surrounding brightness. Our goal is to minimize the absolute value of the difference

$$d_i = m_i^\oplus - m_i^\ominus, \quad (15)$$

i.e., to produce a homogeneous camera image, where the cut-out areas cannot be distinguished from their surrounding test target. This step corresponds to the box “compare” in Fig. 4. To achieve the minimization of  $|d_i|$ , the gray levels of the monitor have to be adjusted at the cut-out positions. Towards this end, the geometric relation between the monitor coordinates of the cut-out areas and the camera coordinates is utilized (see Eqs. (8) and (9)): The regions  $\mathcal{M}_i$ , which have been detected in the camera image and which are therefore given in camera coordinates, are transformed to regions given in monitor coordinates via

$$\mathcal{D}_i(x_{\text{mon}}, y_{\text{mon}}) = \mathcal{M}_i(x_{\text{cam}}, y_{\text{cam}}). \quad (16)$$

The regions  $\mathcal{D}_i$ , which are displayed on the monitor (see Fig. 9), directly correspond to the cut-outs of the calibration target. In other words: When the regions  $\mathcal{D}_i$  are displayed on the monitor and the target in Fig. 2 is applied to the monitor surface, the displayed regions shine through the cut-outs of the calibration target.

In the following, the displayed monitor image is given by  $I_d$ . The differences  $d_i$  between the cut-out areas and their surroundings computed in Eq. (15) can then be used to update the monitor image to produce an image. Towards this end, the image data is updated via

$$I_d^{n+1}(\mathcal{D}_i) = I_d^n(\mathcal{D}_i) + \alpha d_i^n, \quad (17)$$

where  $\alpha$  is a step factor which specifies the speed of convergence (see box “adapt displayed image” in Fig. 4). The variable  $n$  is the



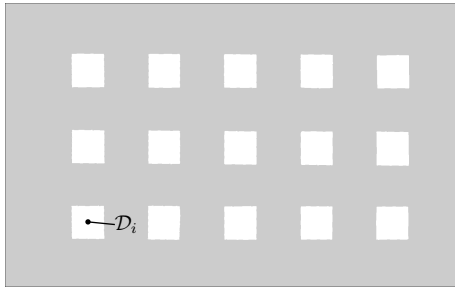


**Figure 9.** Displayed patches  $\mathcal{D}_i$  on the monitor, which have been derived from the camera image in Fig. 7 and which correspond to the cut-out areas  $\mathcal{M}_i$ .

iteration step number and  $d_i^n$  is the difference  $d_i$  in the  $n$ -th step. The term  $I_d(\mathcal{D}_i)$  accesses the region  $\mathcal{D}_i$  in the image  $I_d$ . Eq. (17) increments the image  $I_d$  in the region  $\mathcal{D}_i$  by the values  $\alpha d_i$ . When the differences  $d_i$  are near zero, the adaptation is stopped.

Now an iterative process starts: An actual camera image is acquired and the average pixel values for the different regions are computed via Eqs. (12),(14). The differences of the pixel values between the areas inside and outside the cut-out areas are computed via Eq. (15) and, again, the image is updated via Eq. (17). The iterative approach allows a monitor calibration regardless of non-linear brightness relations between camera and monitor.

## Results

We use an Apple Cinema Display with 20 inch diagonal and a resolution of  $1680 \times 1050$  pixel. The camera aiming at the display is the Allied Vision Technologies camera “Dolphin” which features a resolution of  $1392 \times 1038$  pixel. It is mounted on a tripod and is approximately positioned as shown in Fig. 2. The acquisition and image processing is performed with Mathworks Matlab<sup>®</sup>. The homogeneity calibration mask is build with paper showing hardly any fluorescence and is back-glued with an opaque material. The structuring element  $F_1$  in Eq. (11) is a rectangular  $13 \times 13$  filter kernel and the structuring element  $F_2$  in Eq. (13) is a rectangular  $25 \times 25$  kernel.

Fig. 10 shows the acquired image of the final calibrated monitor: The cut-outs can be hardly located by their edges, because the brightness of the cut-out areas shown on the monitor perfectly matches the brightness of the corresponding surrounding areas illuminated by the external light source. By performing a color transformation, the obtained calibration can then be transferred to human viewers as shown in section “Background and Model”.

The gray levels of the monitor which have been used to produce the image in Fig. 10 are shown in Fig. 11. A slight increase from the left to the right side of the monitor can be noticed. The gray levels shown in Fig. 11 are then used to compute the brightness compensation mask in Fig. 12. This mask is applied to images before they are displayed on the monitor.

Fig. 13 shows the remaining differences between the camera values inside and outside the cut-out areas (see Fig. 8). Since the camera values obtained via Eq. (12) and Eq. (14) are averaged over an area of a certain size, the values given in the diagram are not integer values. The remaining differences except for the large area “1” are all below 2 digits (8 bit) and indicate a successful calibration. A limitation of the accuracy is given by the quantization of the transmission channel between the graphics card and the monitor, which is only 8 bit.



**Figure 10.** Acquired image of the calibrated monitor with the calibration mask applied; the brightness of the monitor cut-out areas perfectly match with their surrounding brightness values. Therefore, the mask can hardly be identified.

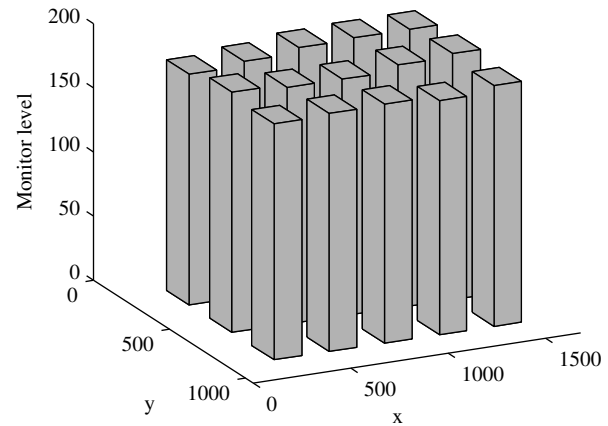


**Figure 11.** Calibrated monitor gray levels at the cut-out areas shown in Fig. 7; the gray levels increase from the left to the right side.

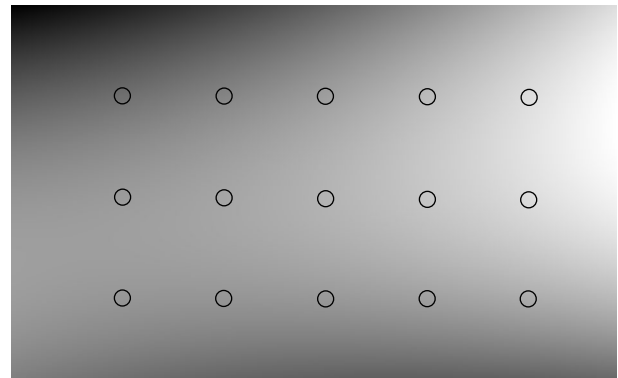


**Figure 12.** Brightness compensation mask (scaled) computed from the data points shown in Fig. 11.

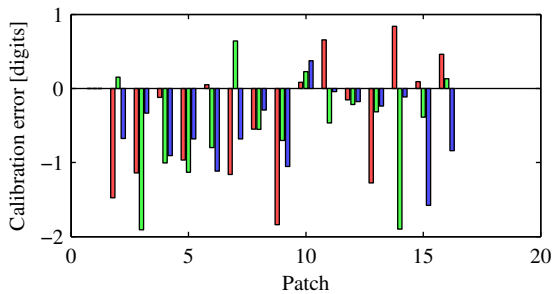


**Figure 13.** Calibration error: Remaining difference  $d_i$  between camera values inside/outside cut-out areas (see Fig. 8).

## Conclusions

A calibration method for brightness homogenization of the monitor with respect to a template in front of the monitor has been presented. The automatic algorithm only requires a grayscale or RGB camera and an opaque template mask with several cut-outs. The cut-outs may exhibit an arbitrary form, the calibration algorithm automatically adapts to this form. Also, the alignment of the camera and the monitor is uncritical, since the proposed method computes a transformation accounting for misalignments. By applying the algorithm a perfect matching between the cut-out areas of the monitor and the surrounding areas can be achieved. Therefore, objects placed in front of the monitor can be compared side-by-side with their reproduction on the monitor.

In the future, we plan to account for the geometric distortions of the camera image. At this time, we use a lens which does not exhibit large distortions.

## References

- [1] T. H. Ha, S. Srivastava, E. J. Delp, and J. P. Allebach, "Monitor characterization model using multiple non-square matrices for better accuracy," in *Proc. IS&T/SID 17th Color Imaging Conference (CIC)*, pp. 117–122, (Albuquerque, NM, USA), Nov 2009.
- [2] E. A. Day, L. Taplin, and R. S. Berns, "Colorimetric characterisation of a computer-controlled liquid crystal display," *Color Research and Application* **29**, pp. 365–373, Oct 2004.
- [3] B. Hill, "Softproofing system for accurate colour matching and study of observer metamerism," in *Proc. IS&T's 5th European Conference on Color in Graphics, Imaging, and Vision (CGIV)*, (Joensuu, Finland), June 2010.
- [4] B. Hill, S. Helling, and A. Glowinski, "Verfahren und Vorrichtung zur originalgetreuen Wiedergabe von Farben auf Bildschirmen," 2008. German Patent DE 10 2008 021 148.6.
- [5] G. Wyszecki and W. S. Stiles, *Color Science: Concepts and Methods, Quantitative Data and Formulae*, Wiley, 1982.
- [6] N. Otsu, "A threshold selection method from grey level histograms," *IEEE Transactions on Systems, Man, and Cybernetics* **9**, pp. 62–66, 1979.
- [7] R. C. Gonzalez and R. E. Woods, *Digital Image Processing (3rd Edition)*, Prentice-Hall, Inc., Upper Saddle River, New Jersey, USA, 2006.
- [8] D. A. Forsyth and J. Ponce, *Computer Vision: A Modern Approach*, Prentice Hall, Aug 2002.

## Author Biography

Johannes Brauers received his diploma degree in Electrical Engineering from RWTH Aachen University, Germany, in 2005. Since then he is with the Institute of Imaging and Computer Vision, RWTH Aachen University as a Ph.D. student. His current research interests are multispectral imaging, in particular modeling and compensation of geometric distortions, high dynamic range imaging and monitor calibration. He received the "EADS Defence Electronics ARGUS Award 2005" for his master thesis and the "Best Student Paper Award" at the IS&T/SPIE International Conference on Digital Photography VI.

Julie Klein received her diploma degree in electrical engineering and information technology from the Technische Universität München, Germany, and her engineering diploma degree from the Ecole Centrale Marseille, France, in 2008. Since then, she has been working at the Institute of Imaging and Computer Vision, RWTH Aachen University, as a Ph.D. student. Her work focuses on multispectral imaging, in particular the analysis and the compensation of aberrations in multispectral cameras.

Bernhard Hill received his diploma and Dr.-degree in Electrical Engineering from the RWTH Aachen University in Germany in 1964 and 1968, respectively. In 1969, he joined the Philips Research Laboratory Hamburg, Germany. In 1984, he changed to the University in Aachen and was appointed professor and head of a research institute. He retired in 2005, but continued research in multispectral imaging and color reproduction. He was general chair of CGIV 2004, held in Aachen. He is a member of IS&T, VDE and DfwG in Germany.

Til Aach is Head of the Institute of Imaging and Computer Vision, RWTH Aachen University. From 1993 to 1998, he was with Philips Research Laboratories. From 1998 to 2004, he was a Full Professor and Director of the Institute for Signal Processing, University of Luebeck, Germany. His research interests are in medical and industrial image processing, signal processing, pattern recognition, and computer vision. He has authored or co-authored over 200 papers, and is a co-inventor for about 20 patents.